Synthesis and Linear Viscoelastic Behavior of Poly(amic acid)–Organoclay Hybrid

JONGKWAN KIM,[1] RIAZ AHMED,[2] SEUNG JONG LEE[1]

[1] School of Chemical Engineering, Seoul National University, Seoul 151-744, Korea

[2] Department of Applied Chemistry, University of Karachi, Karachi 75270, Pakistan

Received 12 January 2000; accepted 3 July 2000

ABSTRACT: Synthesis and rheology of poly(amic acid)–organoclay hybrids were studied in order to address the molecular chain ordering and its relationship with clay particles in the prepolymer. The poly(amic acid) was prepared from oxydianiline and pyromellitic dianhydride solution in N-methylpyrollidinone with exfoliated montmorillonite. The composite solution was mixed to the nanoscale level, and the extent of defoliation and phase separation were studied using X-ray diffraction, transmission electron microscopy, and differential scanning calorimetry. Linear viscoelasticity was used to examine the influence of increasing extent of organoclay. The gelation time of the prepolymer decreased exponentially with increasing clay content. Scaling behavior by power law frequency independence at gel point was found ($G' \propto G'' \propto \omega''$) from slopes of storage and loss moduli. The power law exponent n was found to be about 0.5. At low organoclay concentrations, the gel becomes stiffer and gel strength rises with the concentration. At higher concentrations, the gel becomes weak, gel strength decreases, and phase separation seems to take place, possibly due to organoclay aggregation. The study suggests that linear viscoelasticity can be used to understand the evolution of molecular order in prepolymers of polyimide and its clay hybrids. © 2001 John Wiley & Sons, Inc. J Appl Polym Sci 80: 592–603, 2001

Key words: polyimide; linear viscoelasticity; gelation; montmorillonite; organoclay

INTRODUCTION

Polyimides, comprising planar rigid groups interconnected through fixed bond angles, exhibit less chain flexibility resulting in high softening temperature, thermal resistance, and mechanical properties. Thus polyimides are one of the most frequently used polymers in microelectronics, employed as high-temperature insulators and dielectrics.[1,2] Addition of smectic organophilic clay has been reported to improve gas barrier and thermal expansion properties of rigid polyimide even further. Clay minerals consisting of stacked silicate sheets of nanometer dimension, as montmorillonite, have been extensively used in making of clay–polymer hybrids.[3–7] Polyimide–montmorillonite hybrids were initially synthesized by Yano *et al.*[8,9] and Lan *et al.*[10] from poly(4,4′-oxydiphenylenepyromellitamic acid).

Formation of polyimide or clay–polyimide systems from poly(amic acid) shows a phase transition behavior[11] as the homogeneous solution of the dianhydride and amine gels and solidifies into an imide as a function of time or temperature or both. Phase transitions often show scaling behav-

Correspondence to: Seung Jong Lee (sjlee@plaza.snu.ac.kr).

Contract grant sponsor: Brain Korea 21 Project.

Journal of Applied Polymer Science, Vol. 80, 592–603 (2001)

ior as a function of main physical properties.[12] The scaling theory[13] assumes that the characteristic properties are self-similar functions of independent variables. From a mathematical point of view, self-similarity implies scaling through power-law dependence. In the last decade, dynamic mechanical experiments have been used to obtain intermediate models of viscoelasticity,[14,15] which generalize the classical spring and dashpot models[16–18] and reduce them to scaling laws. Application of such scaling laws to the earlier stages of phase transition in prepolymers of polyimide and clay hybrids are of interest here.

Semicrystalline polymers have been reported to respond sensitively to early stages of molecular ordering during crystallization[19,20] and such early stages can be modeled as a physical gelation process.[21] In such cases motions of groups of molecules correlate and the divergence of growing correlation length is considered as physical gel point. Using crosslinking polymers, initially Winter used scaling laws to develop a mechanical definition of the gel point[22] for chemical gels. The resulting linear viscoelastic gel equation has a finite strain measure that relates the instantaneous stress tensor with the strain history[23–25]:

$$\sigma(t) = -S \int_{-\infty}^{t} (t - t')^{-n} \frac{\partial}{\partial t'} (C^{-1}(t'))\, dt' \qquad (1)$$

where $\sigma(t)$ is the stress tensor, C^{-1} (t') is the Finger strain tensor and its gradient applicable in the range of $-\infty < t' < t$, t and t' are the present and past times, S is the gel strength parameter, and n is the relaxation exponent. Stoichiometrically balanced end-linking networks were found initially to relax with $n = 0.5$,[23] while stoichiometrically unbalanced networks relax with n in the range of $0 < n < 1$.[24] Therefore, experimentally n is not constant and is related to the specific nature of each gelling system.[26] With two material parameters, S and n, the linear viscoelastic behavior at the gel point, as found in chemical gels, can also be applied to physical gels.[21]

Equation (1) is applicable to shear flow gel point on the basis of the assumption that the linear viscoelastic oscillatory shear storage, $G'(\omega)$, and loss, $G''(\omega)$, moduli are congruent, and is described by the scaling relation:

$$G'(\omega) \propto G''(\omega) \propto \omega^n \qquad (2)$$

Using the Boltzmann superposition principle,[22] the storage and loss moduli of the complex shear modulus G^* are related to the time-dependent modulus of linear viscoelasticity via the following Fourier transform:

$$G^* = i\omega \int_0^{\infty} \exp(-i\omega t) G(t)\, dt \qquad (3)$$

Thus, at gel point in oscillatory shear, the dynamic moduli represent a scaling relationship with frequency

$$G' = \frac{G''}{\tan \delta} = S\Gamma(1 - n)\omega^n \cos \delta \qquad (4)$$

where $\Gamma(1 - n)$ is the γ function and is the phase angle in linear viscoelasticity. As a consequence of power-law dynamics, the loss tangent should be frequency independent and proportional to the relaxation exponent[21,27–29]:

$$\tan \delta = \tan\left(\frac{n\pi}{2}\right) \qquad (5)$$

It has been shown that a power-law stress relaxation behavior depicts the fractal time behavior implying processes without a characteristic time scale.[30] Thus Winter's scaling law has been used to probe the cluster size during gelation. The relaxation exponent is linked to the self-similar fractal dimension near the gelation threshold and in some cases it is found that the stoichiometric ratio or the crosslinker content influence the relaxation exponent and thus fractal geometry.[30–32] The aim of this paper is to develop an understanding of the molecular ordering process in the prepolymer, poly(amic acid), involving organophilic clay with the help of the self-similar scaling law as the prepolymer evolves into a highly ordered polyimide–organoclay hybrid.

In this work, X-ray diffraction (XRD) and transmission electron microscopy (TEM) were carried out to determine the dispersion of clay in polymer matrix. Differential scanning calorimetry (DSC) was performed to study the effect of clay on imidization condition (temperature, heat of reaction). Oscillatory shear measurements were made to examine how the clay affects the rheological characteristics, such as the gelation time and the gel strength.

EXPERIMENTAL

Materials

Organically modified montmorillonite, Cloisite 30B, which has organic salt of di-tallow methyl

dihydroxyethyl ammonium, average dry particle size of less than 13 μ, and 53% inorganic content, was provided by Southern Clay Products. The two hydroxyethyl groups lend polarity compatible to polyimide (polar) solvents. 4,4′-Oxydianiline (ODA), pyromellitic dianhydride (PMDA), and the polar solvent N-methyl-2-pyrrolidinone (NMP) were purchased from Aldrich Chemical Co.

Preparation of Polyimide–Oragnoclay Hybrid

The polymer–organoclay hybrid containing 1% organoclay was prepared following the method of Yano et al.[8,9] with slight modification of the solvent as instead of dimethylacetamide, NMP was used. The amount of 2.01g of organoclay and 27.99 g of NMP were stirred by an impeller mixer at 90°C for 1 h, thus providing a well-dispersed and stable 6.7% NMP dispersion of organoclay. NMP solution of poly(amic acid), poly(4.4′-oxydiphenylenepyromellitamic acid), was prepared by mixing 15.36 g of NMP and 1.47 g of ODA at 30°C for 30 min, adding 1.54 g of PMDA to this solution, and stirring for 1 h. Next, 0.42 g of the NMP dispersion of organoclay was added to the previous solution and stirred at 30°C for 4 h to obtain poly(amic acid)–organoclay solution (PAA).

Three grams of the poly(amic acid)–organoclay solution was spread on a glass dish and heated at 60°C for 30 min and at 95°C for 90 min under 76 mm Hg in a vacuum oven, resulting in a 0.05 mm film of poly(amic acid)–organoclay hybrid (PAAF). Precure at 95°C ensures that the decomplexation usually found in poly(amic acid) films prepared at low cure temperatures was suppressed.[33] Curing at 95°C also places the molar ratio of the solvent NMP to less than one,[33,34] and thus there is around 30%[35] free NMP left in the sample to allow "plasticization" of the poly(amic acid) once decomplexed. Alternatively, the PAAF films were additionally cured at 250°C for 30 min under nitrogen to obtain polyimide (PI), poly(4,4′-oxydiphenylenepyromellitimide). The composition of organoclay in PAA and PAAF is shown in Table I.

Table I Composition of Organoclay in Poly(amic acid)–Oragoclay Solutions (PAA) and Poly(amic acid)–Organoclay Films (PAAF)

Organoclay in PAA (%)	Organoclay in PAAF (%)
0.00	0.0
0.15	1.0
0.30	2.0
0.97	6.0
1.51	9.0
2.24	14.0

Characterization

XRD was carried out on PAAF and PI using a Rigaku D/MAX-IIIC X-ray Diffractometer (40 kV, 45 mA) with Cu-Kα in transmission mode. TEM was conducted using Jeol JEM-2000EXII at an acceleration voltage of 200 kV. The TEM carbon-coated copper grids were coated with poly(amic acid)–organoclay hybrid and cured at conditions listed above for imidization. DSC analysis of the clay–polyimide hybrid was performed with DSC 2010 of TA Instruments. Two milligrams of PAAF was equilibrated for 30 min at 25°C followed by heating runs between 25 and 350°C at 10°C/min.

Oscillatory shear measurements were performed on a Rheometrics Mechanical Spectrometer RMS-800 with a modified cup and plate geometry having a 25 mm diameter ringed lower plate, which prevents the PAA from flowing out. To correct for the ring, a correction factor can be used.[36] Oscillatory shear time sweep experiments were performed at a frequency of 0.1rad/s and strain of 1.25%. Frequency sweep experiments were carried out at a 1.25% strain in a frequency window of 0.01–100 rad/s at 50°C. Experiments were performed at 50°C, which involves the ring opening process in the conversion of the anhydride and amine into poly(amic acid). Condensation at elevated temperatures prevents rheological measurements under such conditions.

RESULTS AND DISCUSSION

X-Ray Diffraction

Figure 1 shows the X-ray diffraction curves of pure polyimide, PAAF hybrids containing 1-14% organoclay, and the organoclay (Cloisite 30B) powder. Clay powder shows a 001 peak at $2\theta = 4.8°$ corresponding to an interlayer spacing of $d = 18.3$ Å; however, the hybrids show no 001 peak. Absence of 001 and subsequent peaks is interpreted as homogeneous defoliation and dispersion of silicate layers into the polyimide matrix.[8,9,37]

Pure polyimide has a characteristic peak between 6.1° and 6.5° in the 2θ range of 3°–10°. Though hybrids show no clay peak, another peak

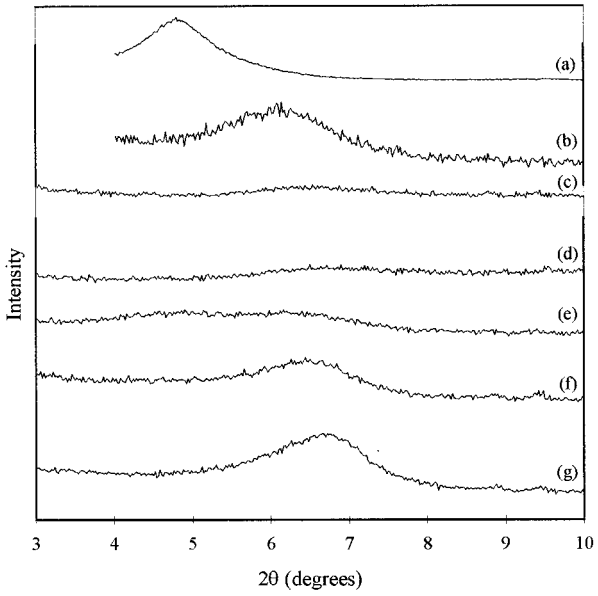

Figure 1 X-ray diffraction curves at $2\theta = 3°–10°$ for (a) organoclay, Closite 30B, (b) pure polyimide, and hybrids with (c) 1, (d) 2, (e) 6, (f) 9, and (g) 14% organoclay.

reappears in 9 and 14% hybrids. This indicates clay disperses into the polyimide matrix but at higher concentrations a possible realignment or reemergence of polyimide structure takes place. Results, similar to ours, can also be seen in the study by Yano et al.,[8,9] though their conclusions are different. This reappearance can be due to relamination of the silicate layers or due to the ordering of PI chains. The latter possibility would imply that the 2θ peak at 6.1°–6.5°, or a d spacing of 13–14 Å, corresponds to the repeat distance along the preferred orientation of the molecular chain within PAAF. This preferred orientation in the PAAF also retains in the PI,[35] and our results, though not reported here, show the same. It can be concluded that a small amount of clay tends to suppress the small angle 2θ peak of polyimide that reappears at larger additions.

Figure 2 shows XRD of polyimide, organoclay, and 1% organoclay hybrid in the region from 2θ =10°–100°. The 002 and subsequent peaks of clay disappear in 1% hybrid. However, in the PAAF amorphous halo[35,38] peak remains. This is characteristic of isotropic orientation and the absence of crystalline order.

Transmission Electron Microscopy

A transmission electron micrograph of 2% organoclay hybrid film is shown in Figure 3(a) where the dark lines are clay layers. This micrograph shows layers of clay are dispersed homogeneously into the polyimide matrix.

Figure 3(b), a micrograph of 14% organoclay hybrid, however, shows two phases. One phase consists of the aggregation of defoliated layers into a separate phase also containing polyimide. The other phase appears as pure polyimide. These separations may explain the reemergence of the polyimide XRD peaks in hybrids of higher concentration. They also help us understand why no clay peak is found in XRD of highly concentrated hybrids because the aggregated (clay–polyimide separated) phase still contains defoliated layers. On the other hand, the appearance or suppression of the small angle polyimide peak led Yano et al.[8,9] to conclude incomplete dispersion from a peak at d = 17.6 Å due to aliphatic chain incompatibility. But our XRD results showed a polyimide peak at d = 14 Å, also corroborated from our TEM results. Therefore, we can conclude that clay layers aggregated and formed a clay–polyimide separated phase. As a result, the hybrids of higher concentration tend to show resurgence of polyimide 6.1°–6.5° peak.

Differential Scanning Calorimetry

Imidization peak temperatures obtained from DSC traces of PAA and 1~14% organoclay PAAF hybrids are shown in Figure 4. The imidization

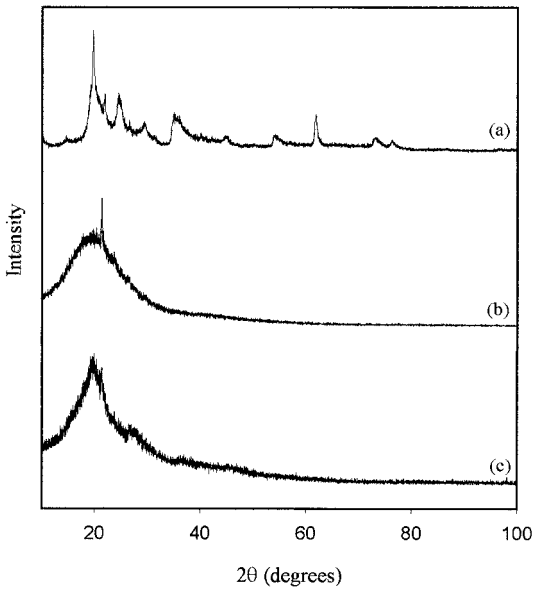

Figure 2 X-ray diffraction curves at $2\theta = 10°–100°$ for (a) organoclay, Closite 30B, (b) pure polyimide, and (c) 1% organoclay hybrid.

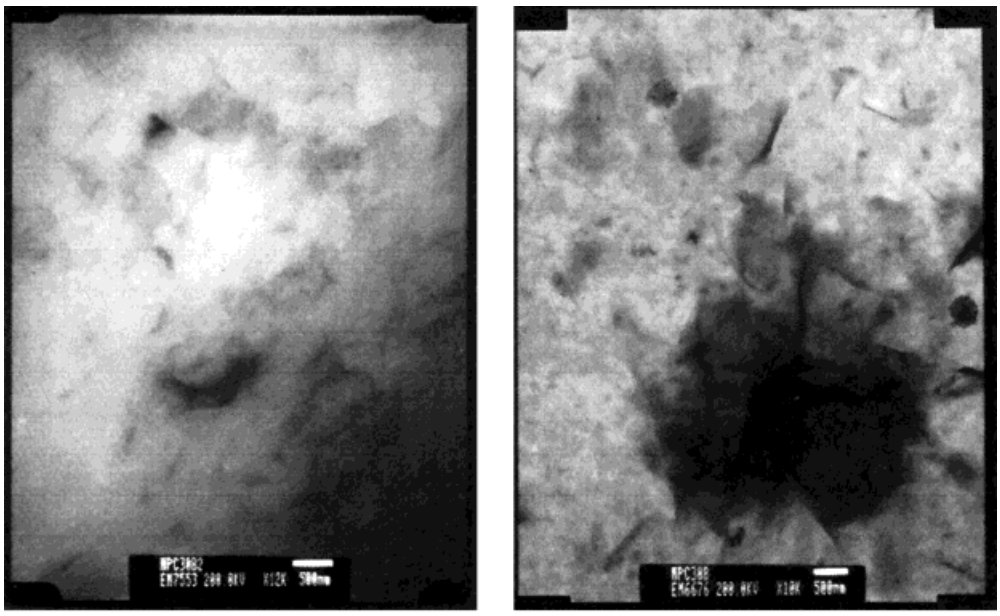

(a) (b)

Figure 3 Transmission electron micrograph of polyimide–organoclay hybrid films at (a) 2 and (b) 14% organoclay concentrations.

temperature T_i, usually characterized by a peak in the imidization curve, shows little variation with clay content. T_i is nearly constant with respect to clay concentration. This indicates molecular architecture of hybrid is not changed by clay addition. Usually, T_i changes if the molecular structure is changed.

The reaction enthalpy ΔH was calculated from the start of the imidization temperature. In contrast to T_i, ΔH decreases exponentially with increasing clay content (Fig. 4), and seems to suggest that imidization reaction and molecular ordering is influenced by clay. This result can be explained as follows.

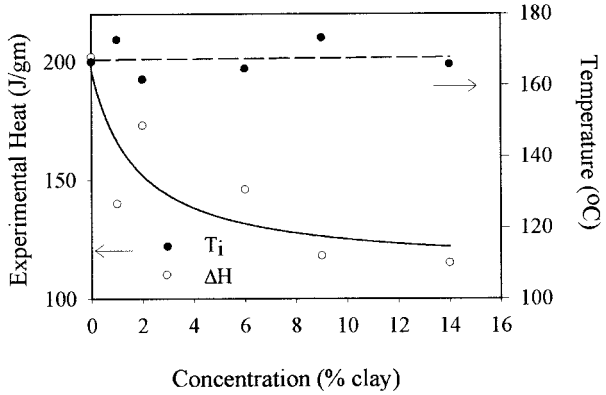

Figure 4 Experiments heat of reaction ΔH and imidization temperature T_i vs organoclay concentration during imidization of poly(amic acid) and its hybrids.

The exfoliated silicate layers provide large surface area as active sites for promoting the dehydration and imide ring closure reaction.[37] In other words, the modified clay appears to act as a catalyst promoting the reaction rate. Fourier transform infrared analysis on the PMDA–ODA–clay system has been shown to improve reaction rates up to 7% of clay concentration.[37] Our activation energy calculations from thermograms show similar results. Beyond 6–8% there is not much improvement in the heat of reaction or rate of imidization. Instead, the decline in ΔH indicates that additional clay particles hinder strong molecular ordering of PAAF. Our results with clay seem to suggest an increased obstruction to crystallization during imidization that is in addition to the structural irregularity attributed to the *para* and *meta* pyromellitamic units along the PAAF chain.[35,39]

The decrease in ΔH found in this study is analogous to the effect of high molecular weight linear

chains when blended into a short chain crosslinking system, a rod-like polyimide containing a benzhydrol unit.[40] Bulky substituents to the polyimide ring reduce intermolecular forces between imide chains due to looser packing; therefore the tendency to crystallize is lowered. Substituents create steric effect hindering dense packing and acting as spacers for the polymer molecule.[40]

Though the reaction rate is improved, the clay does not change polyimide molecular structure. Scanning calorimetry results are being taken increasingly as a confirmation test for clay–polymer structure on the nanoscale[41,42]; especially, the disappearance of the melting peak is taken to establish formation of what is called a nanocomposite. For example, it has also been reported for polystyrene[41] and polyethylene oxide nanocomposites[43] that the glass transition peak disappears due to inhibition caused by inorganic layers restricting large domain formation. Thus a clay–hybrid study[44] reports that melting temperature T_m and heat of fusion decrease with increasing clay content. Also, ΔH_m is shown to have a very weak relationship with clay content. Another study,[45] shows that ΔH_m decreases with increasing clay content and T_m is nearly constant. It should be pointed that these studies involve thermoplasts, and ΔH_m is based upon the melting process, while our study concerns an imidization reaction leading to an highly ordered state of extended chains in PAAF imidizing to become PI. In other words, our imidization peak is not melting peak but instead represents the molecular chain ordering.

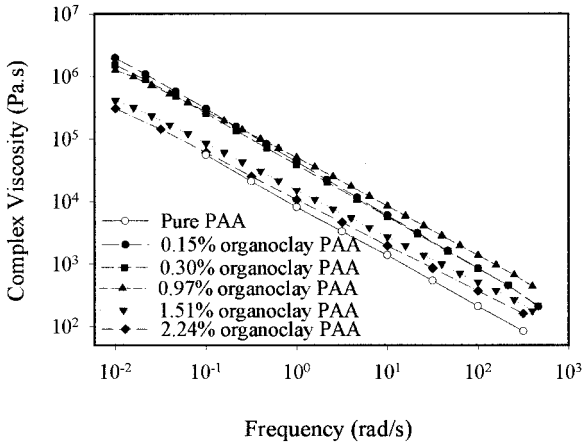

Figure 5 Complex viscosity vs frequency for pure PAA and organoclay PAAs at different concentrations at 50°C after 7200 s in linear viscoelastic oscillatory shear time sweep at 1.25% strain and 0.1 rad/s frequency.

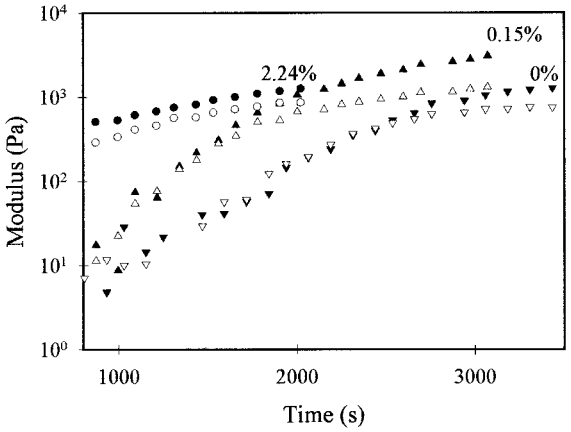

Figure 6 Oscillatory shear storage modulus (filled symbols) and loss modulus (unfilled symbols) vs time measured at 50°C, 1.25% strain and 0.1 rad/s frequency for pure PAA, 0.15 and 2.24% organoclay PAA.

Rheology

The complex viscosity, obtained from linear oscillatory shear, after a time sweep of 2 h for various organoclay PAAs, is shown in Figure 5. Extreme shear thinning behavior with a power-law index of 0.2–0.3 indicates that at 50°C the gels are still weak enough to yield at high shear. It is interesting that an over 1.5% clay concentration the organoclay PAA shows lower viscosity similar to the pure PAA. A time sweep of pure 0.15 and 2.24% organoclay PAA at 50°C shows crossover in G' and G'' for low concentrations (Fig. 6). A relatively low temperature was chosen to obtain a large time range for experiments. We try to address the linear viscoelastic behavior in terms of the gel point.

Chambon and Winter[22] used the evolving relaxation time spectrum and universality for rheological behavior at the gel point. This implies the self-similarity of the structure, linked to linear viscoelastic moduli, follows power law in a frequency sweep experiment. By universality it means that both physically and chemically crosslinking materials can be described in terms of solution–gel dynamics.

An accurate estimation of the gel point and relaxation behavior as expressed in the relaxation exponent n for chemically or physically gelling systems can be made by a frequency-independent value of tanδ obtained from a multifrequency plot against gelation time, temperature, or concentration of the reactants.[19, 25, 46] An alternative, and equivalently accurate, method is the estimation of

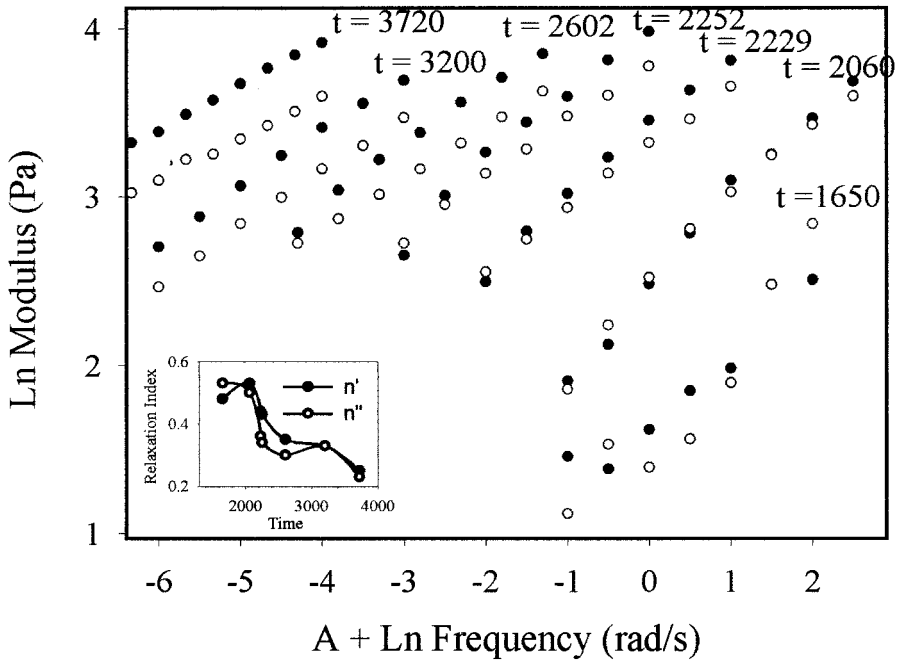

(a)

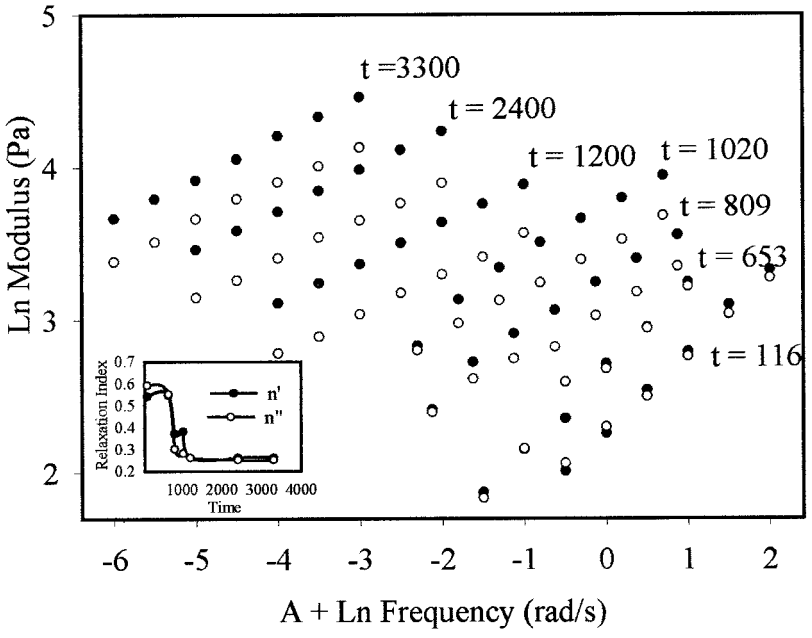

(b)

Figure 7

slope of $G'(\omega)$ and $G''(\omega)$ curve, and plotting the slopes n' and n'' at various pre- and postgel stages. Figures 7(a)–(c) show results of frequency sweep experiments performed at various stages of gelation for pure and organoclay hybrids. The congruency of G' (ω) and $G''(\omega)$ at shorter times shows the applicability of Winter's criteria, and allows the calculation of Winter's power-law index n and the gelation time.

The gel point (time) is obtained when the calculated n' and n'' crossover at a single point.[47] Being a stoichiometrically balanced system,[25,47]

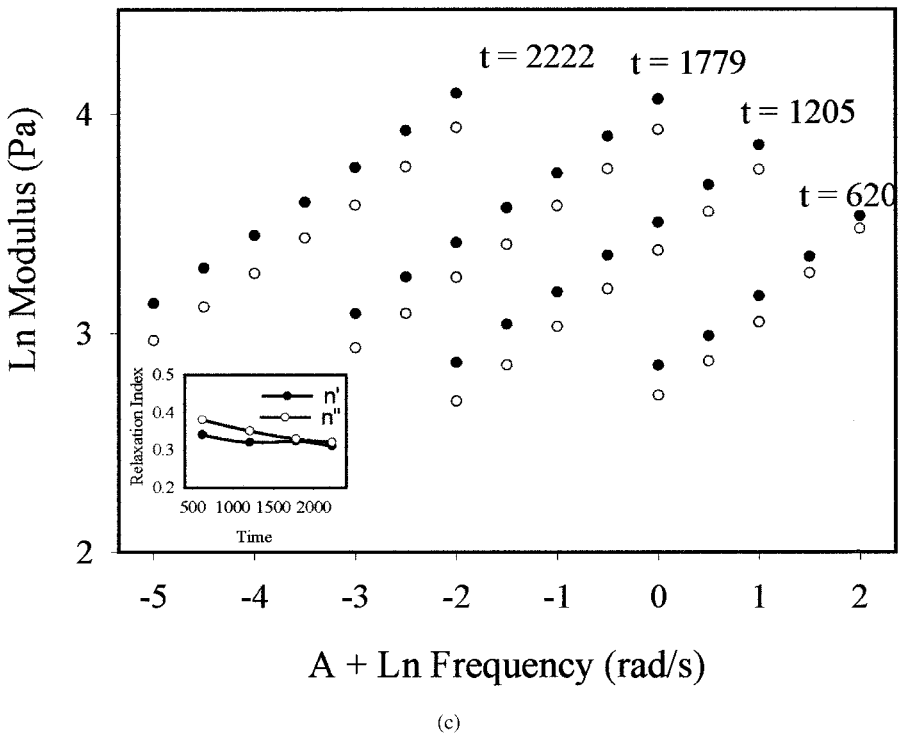

(c)

Figure 7 (a) $G'(\omega)$, filled symbols, and $G''(\omega)$, unfilled symbols, vs frequency at various curing times for pure PAA. Data shifted: $t = 1650, A = 0$; $t = 2060, A = 0$; $t = 2229, A = 10^{-1}$; $t = 2252, A = 10^{-2}$; $t = 2602, A = 5 \times 10^{-4}$; $t = 3200, A = 10^{-4}$; $t = 3720, A = 10^{-5}$. Inset shows the slope n' and n'' against time. (b) $G'(\omega)$ and $G''(\omega)$ vs frequency at various curing times for 0.3% organoclay PAA. Data shifted: $t = 116, A = 0$; $t = 653, A = 10^{-1}$; $t = 809, A = 7.5 \times 10^{-2}$; $t = 1020, A = 5 \times 10^{-3}$; $t = 1200, A = 10^{-3}$; $t = 2400, A = 10^{-4}$; $t = 3300, A = 10^{-5}$. Inset shows the slope n' and n'' against time. (c) $G'(\omega)$ and $G''(\omega)$ vs frequency at various curing times for 2.24% organoclay PAA. Data shifted: $t = 620, A = 0$; $t = 1205, A = 10^{-1}$; $t = 1779, A = 10^{-2}$; $t = 2222, A = 10^{-4}$. Inset shows the slope n' and n'' against time.

the gel point is obtained, in all cases except 2.42% hybrid, near the crossover in $G'(t)$, $G''(t)$ curves, as shown in insets to Figures 7(a)–(c). Similarly, the gelation time was obtained for various clay concentrations [Fig. 8(a)]. The decay is exponential with increase in clay content, that implies a small amount of organoclay drastically decreases the gelation time.

The power-law index remains around 0.5 up to 1.5% organoclay in the PAA [Fig. 8(b]. Similar values have been reported for polydimethylsiloxane[24] and polyurethane.[23] The value of n is theoretically to vary between 0 and 1 as the phase angle in linear viscoelasticity experiment varies from 0 to $\pi/2$. This helps characterize the rheology from being purely viscous to purely elastic solid.[26] The n depends on the molecular characteristics, stoichiometric ratio, and gelation conditions.[48] In the case of the poly(amic-acid)–organoclay hybrid, the stoichiometric concentration of the prepolymer (oxydianiline and dianhydride) was kept constant; the amount of solvent was also kept the same. The percentage of organoclay was increased from 0 to 2.24 in order to observe the influence of organoclay on the PAA.

Various interpretations of the power-law index have appeared in literature[31,32,49–51] Short chains are supposed to give n around 0.7 and long chains around 0.5.[31] The nonuniversality of n has been related to intermolecular interactions such as entanglements and branching, which are ignored instead due to mathematical complexity.[48] The n has been found to depend on the molecular weight in particular.[52] The reduction in n can imply increasing fractal size.[32,47,48]

It has been reported that decrease in n may arise due to presence of silicate fillers providing physical crosslinks existing for a finite life time at

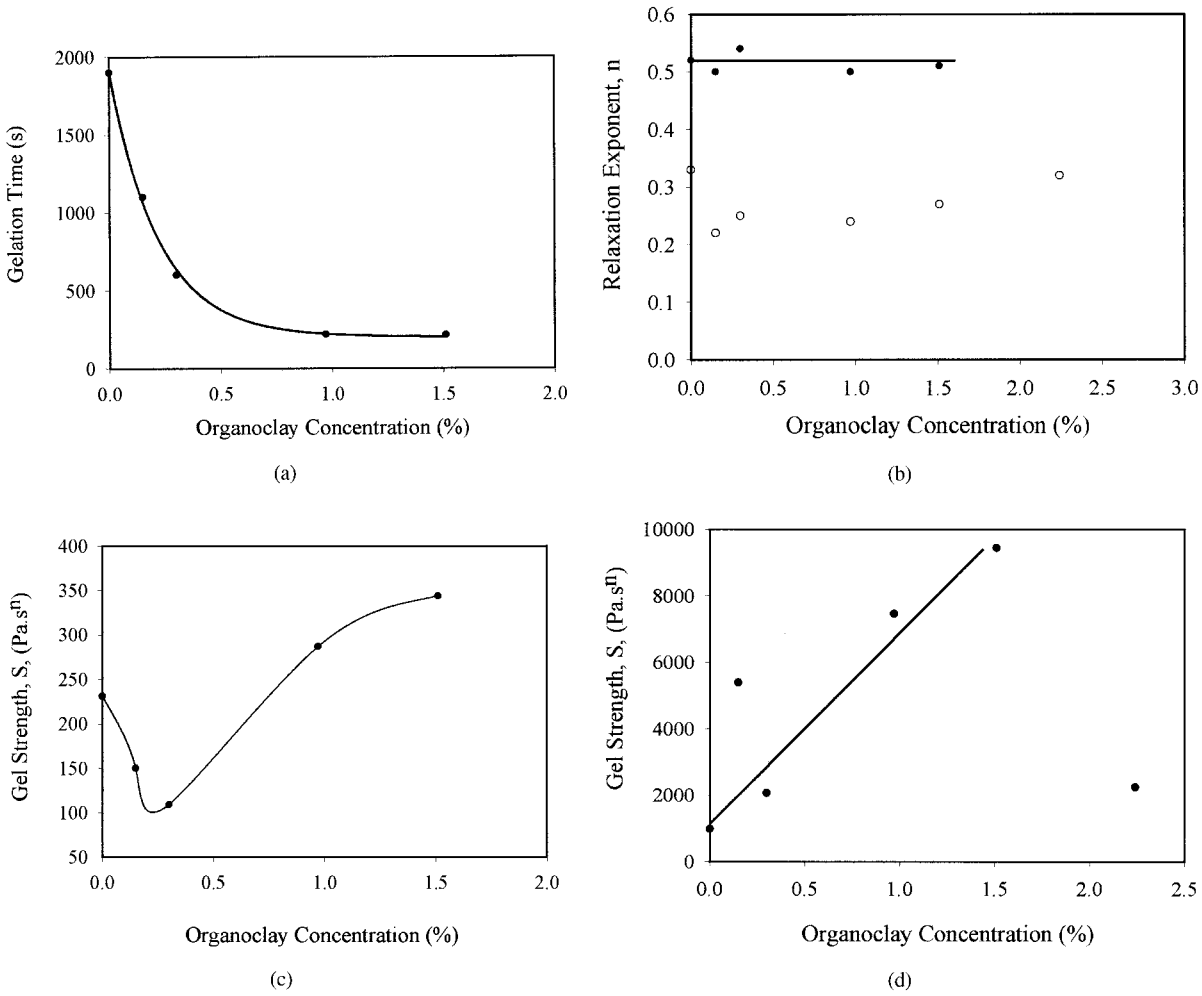

Figure 8 (a) Gelation time versus organoclay concentration in PAA. (b). Relaxation exponent n vs organoclay concentration in PAA. Black circles are for gelation time from $G'(\omega)$ and $G''(\omega)$ congruency and open symbols are from gelation time for critical gel. (c) Gel strength S vs organoclay concentration in PAA with relaxation exponent calculated from congruent frequency sweep data. (d) Gel strength S versus organoclay concentration in PAA with relaxation exponent calculated from critical gel estimates.

the gel point thus creating a denser structure.[49] Studies on chemical gels show that concentration of both the polymer and the crosslinking agent influence n and S.[27,47] For chemical gels in crosslinking systems[26] higher polymer or crosslinker concentration are reported to enhance entanglement and thus decrease n. At fixed polymer concentration, the rise in crosslinker also reduces n.[47] Essentially, there is little evidence that actual cross-linking takes place even in imidization of PAAF into PI films at higher temperatures.[53,54]

Usually fillers and crosslinking agents increase gel strength up to a certain limit. Additions beyond that limit do not improve gel strength but also do not decrease the gel strength.[23,47] This issue can be addressed by examining the gel strength parameter S. From n it is possible to obtain S at a given value of $G'(\omega)$ at the gel point; an average value of the moduli was used to avoid greater errors.[26] Organoclays seem to enhance prepolymer gel strength [Fig. 8(c)].

For chemical gels, with constant n, increasing crosslink density increases the gel strength.[32] Our results are thus consistent with some of chemical gels. The rise indicates that the organoclay improves S. Enhancement of crosslinking density, in addition to entanglement coupling, is related to the increased S for chemical gels[23,32] and thus a "harder" gel is supposed to be formed.[47]

As noted earlier, for the case of high concentration, that is for 2.24% organoclay, the linear viscoelastic time sweep experiment (Fig. 6) does not show a crossover and the storage modulus is higher than the loss modulus right from the beginning of the experiment. In such situations it is customary in gelation rheology to apply the criteria $G' \sim G'' \sim \omega^n$, which means identifying the critical gelation time when slopes of noncongruent $G'(\omega)$ and $G''(\omega)$ are equal.[32,49] We note that application of this criteria is not only possible for 2.24% organoclay hybrids but also for lower clay concentrations and pure PAA. Figure 8(b) also shows the critical gelation relaxation exponent for the pure and organoclay PAAs. As a critical gel, the relaxation index is found to be slightly increasing with clay concentration but still negating existence of crosslinking effect. The gel strength obtained from these exponents is shown in Figure 8(d). Upto 1.5% organoclay PAA, the gel strength rises; however, at 2.24% the strength drops by a quarter, indicating structural rearrangement taking place in the gel. Also, from time sweep experiments (Fig. 6) it appears that the addition of clay improves the short time modulus while at higher concentrations the long time modulus does not improve. In that sense a large amount of organoclay acts as inert substance.

In one study the gel strength has been found to decrease monotonically with increasing concentration of the inert component.[31] As is the case here, high concentrations of inert component has previously been shown to result in rather weaker gels.

In another case of the crosslinking system imbedded with a linear chain polymer, the decrease in gel strength too has been attributed to phase separation.[49] In an earlier section we see from the TEM that at 14% clay in imidized PAAF (2.24% in PAA) the defoliated clay layers tend to aggregate or relaminate with a secondary phase of the polyimide segregating along with the clay layers. It is deduced from the sudden drop in gel strength, observed in the liquid-phase organoclay–PAA, that this aggregation may ultimately show its effect in the solid-phase films as well. The secondary phase acts as a diluent of the primary phase with the aggregated layers unable to resist the flow as much as the low concentration, but defoliated, layers do.

Thus low organoclay concentrations seem to influence the gel strength parameter more than the high concentration where physical junctions increase modulus and provide spectrum dominated by storage moduli though for a finite lifetime.[49] This drastic change in behavior at the gel level also explains why the clay-oriented air and liquid permeation resistance of organoclay[8,9,37] is limited to clay concentrations less than 8% in the imidized films.

For chemical gels,[32,47] an increase in n usually causes a decrease in S; that is not the case in our study. However, lack of clarity exists about the presence[32,49,50] or otherwise[26] of any relationship between n and S. For both physical and chemical gels it is argued that it is not necessary to find a consistent relationship between gel strength and the power law index.[26,55]

In order to explain the features of gels, the fractal nature of critical gels has also been used.[52,56,57] Fractal dimension df relates the radius of gyration and mass of the molecular cluster ($R^{df} \sim M$). The df has been linked to the shrinkage of the size of the polymer with increasing concentration of a dilute solution and increases with increasing secondary linear component in a crosslinking system.[31] It has been postulated for polydisperse solution of polymers that near gel point presence of clusters provides shrinkage of polymer similar to those observed in melts where the excluded volume is fully screened, entanglements are ignored, and Rouse dynamics prevails.[56] For a stoichiometrically balanced system, increasing strand length enhances excluded volume effect; thus the upper bound for n exhibiting screened excluded volume effects is given by[56]

$$n = \frac{d(d + 2 - 2\,df)}{2(d + 2 - df)} \tag{6}$$

where d is the space dimension and df is the fractal dimension.

In the case of organoclay–PAA, the fractal dimension is found near 2 when n is estimated from Winter's congruency criteria. For a 2.42% hybrid, the fractal dimension increases to 2.2. This rise is similar to that observed for crosslinked systems of polyvinyl alcohol systems. The resulting compactness of structure has also been linked to hydrogen bonding in chemical gels,[47] which results in higher df.[56] As observed earlier, the final structure in both amic acid and imide form may be weaker. However the increase in df does not necessarily mean a "tight" structure as observed in some chemical gels.[32,47,51] Beyond 1.5% organoclay, the agglomeration of the defoliated clay particles into a separate phase may give rise in the

fractal dimension, which creates localized dense structure that does not necessarily implies "tightness."

CONCLUSIONS

Synthesis and characterization of poly(amic acid)–organoclay hybrids in solution and film form were carried out to understand the role of organoclay in hybrid formation. The main findings can be summarized as follows: (1) Defoliation of organoclay in poly(amic acid) is possible up to a high concentration of 9% in film; however, large amounts tend to aggregate and phase separate, thus exhibiting an upper bound on clay. (2) Molecular architecture of the resulting hybrid remains similar to that of pure poly(amic acid) though small amounts of organoclay tend to enhance ring opening while large amounts contribute to pyromellitic groups blocking crystallization. (3) Linear viscoelastic measurements indicate that, at the measurement temperature, a weak and reversible structure is formed, which shows shear thinning behavior. (4) Organoclay decreases the gelation time and at low concentration functions similar to crosslinkers. (5) Self-similar power-law behavior is observed at the gelation point, which is found to be independent of frequency. The power-law index remains independent of organoclay content, although at higher concentration clay aggregates with poly(amic acid) leading to phase separation, and thus weaker gel, constraining the structural self-similarity.

We would like to thank the following: Mee Ja Woo of KAIST, Taejon, for XRD experiments; Mee Jong Kang of IUCNSCR, Seoul, for TEM measurements; our mates Hyo Jun Song for help in DSC and Do Hoon Kim for help in rheometry. Our special thanks to Bob Briell of Southern Clay Co., USA, for providing Cloisite 30B and some useful discussions on solvent compatibility. This work was supported by the Brain Korea 21 Project, and Riaz Ahmed would like to thank the Korea Science and Engineering Foundation for the postdoctoral fellowship.

REFERENCES

1. Senturia, S. D. In Polymers for High Technology; Bowden, M. J., Turner, S. R., Eds.; ACS Symposium Series 346; American Chemical Society: Washington, DC, 1987; p 613.
2. Hedrick, J. L.; Carter, K. R.; Labadie, J. W.; Miller, R. D.; Volksen, W.; Hawker, C. J.; Yoon, D. Y.; Russel, T. P.; McGrath, J. E.; Briber, R. M. Adv Polym Sci 1999, 141, 1.
3. Pinnavaia, T. J. Science 1983, 220, 365.
4. U.S. Patent 5164460, 1992.
5. Aranda, P.; Ruiz-Hitzky, E. Chem Mater 1992, 4, 1395.
6. Kojima, Y.; Usuki, A.; Kawasumi, M.; Okada, A.; Kurauchi, T.; Kamigaito, O. J Polym Sci A, Polym Chem 1993, 31, 983.
7. Vaia, R. A.; Giannelis, E. P. Macromolecules 1997, 30, 7990.
8. Yano, K.; Usuki, A.; Okada, A.; Kurauchi, T. Kamigaito, O. J Polym Sci A Polym Chem 1993, 31, 2493.
9. Yano, K.; Usuki, A.; Okada, A. J Polym Sci A, Polym Chem 1997, 35, 2289.
10. Lan, T.; Kaviratna, P. D.; Pinnavaia, T. J. Chem Mater 1994, 6, 573.
11. Bessonov, M. I.; Zubkov, V. A. Polyamic Acids and Polyimides: Synthesis, Transformations, and Structure; CRC Press: London, 1993.
12. Chiaia, B. In Fractals and Fractional Calculus in Continuum Mechanics; Carpinteri, A.; Mainardi, F., Eds.; Springer: New York, 1997.
13. Barenblatt, G. I. Similarity, Self-Similarity and Intermediate Asymptotics; Consultants Bureau: New York, 1979.
14. Bagley, R. L.; Torvik, R. J. J Rheol 1983, 27, 201.
15. Rogers, L. J Rheol 1983, 27, 351.
16. Case, C. M. Fractional Calculus Approach to the Theoretical Description of Viscoelasticity, Desert Research Institute, University of Nevada System, Water Resource Centre, Nevada, No. 41116, 1988.
17. Koeller, R. C. J Appl Mech 1984, 51, 299.
18. Mainardi, F. In Fractals and Fractional Calculus in Continuum Mechanics; Carpinteri, A., Mainardi, F., Eds.; Springer: New York, 1997.
19. Nijenhuis, K.; Winter, H. H. Macromolecules 1989, 22, 411.
20. Nijenhuis, K. Adv Polym Sci 1997, 130, 1.
21. Pogodina, V.; Winter, H. H. Macromolecules 1998, 31, 8164.
22. Chambon, F.; Winter, H. H. Polym Bull 1985, 13, 499.
23. Winter, H. H.; Morganelli, P.; Chambon, F. Macromolecules 1988, 21, 532.
24. Winter, H. H.; Chambon, F. J Rheol 1986, 30, 367.
25. Chambon, F.; Winter, H. H. J Rheol 1987, 31, 683.
26. Li, L.; Aoki, Y. Macromolecules 1997, 30, 7835.
27. Koike, A.; Nemoto, N.; Takashi, M.; Osaki, K. Polymer 1994, 35, 3005.
28. Mours, M.; Winter, H. H. Macromolecules 1996, 29, 7221.
29. Vilgis, T. A.; Winter, H. H. Colloid Polym Sci 1988, 266, 494.
30. Vlassopoulos, D.; Chira, I.; Loppinet, B.; McGrail, P. T. Rheol Acta 1998, 37, 614.

31. Izuka, A.; Winter, H. H.; Hashimoto, T. Macromolecules 1997, 30, 6158.
32. Scanlan, J. C.; Winter, H. H. Macromolecules 1991, 24, 47.
33. Hsu, T. C.; Liu, Z. L. Prog Appl Polym Sci. 1992, 46, 1821.
34. Brekner, M. J.; Geger, C. J. J Polym Sci A, Polym Chem 1987, 25, 2005.
35. Takahashi, N.; Yoon, D.; Parrish, W. Macromolecules 1984, 17, 2583. 3
36. Hwang, J. G.; Row, C. G.; Hwang, I.; Lee, S. J. I&EC Research 1994, 33, 2377.
37. Tyan, H. L.; Liu, Y. C.; Wei, K. H. Polymer 1999, 40, 4877.
38. Coburn, J. C.; Pottiger, M. T. In Advances in Polyimide Science and Technology; Feger, C., Khojastech, M. M., Hoo, M. S., Eds.; Technomic: Lancaster, PA, 1992; p 360.
39. Birshtein, T. M. Polym Sci USSR 1977, 19, 63.
40. Liaw, D.-J.; Liaw, B.-Y.; Li, L.-J.; Sillion, B.; Mercier, R.; Thiria, R.; Sekiguchi, H. Chem Mater 1998, 10, 734.
41. Weimer, M. W.; Cehn, H.; Giannelis, E. P.; Sogah, D. Y. J Am Chem Soc 1999, 121, 1615.
42. Giannelis, E. P. Adv Mater 1996, 8, 29.
43. Vaia, R. A.; Giannelis, E. P. J Polym Sci B Polym Phys 1997, 35, 59.
44. Messersmith, P. B.; Giannelis, E. P. J Polym Sci A Polym Chem 1995, 33, 1047.
45. Jimenez, G.; Ogata, N.; Kawai, H.; Ogihara, T. J Appl Polym Sci 1997, 64, 2211.
46. Schwittay, C.; Mours, M.; Winter, H. H. Faraday Discuss 1995, 101, 93.
47. Kjoniksen, A.-L.; Nystrom, B. Macromolecules 1996, 29, 5252.
48. Koike, A.; Nemoto, N.; Watanabe, Y.; Osaki, K. Polym J 1996, 28, 942.
49. Raghavan, S. R.; Chen, L. A.; McDowell, C.; Khan, S. A.; Hwang, R. White, S. Polymer 1996, 37, 5869.
50. de Rosa, M. E.; Winter, H. H. Rheol Acta 1994, 33, 220.
51. Izuka, A.; Winter, H. H.; Hashimoto, T. Macromolecules 1994, 27, 6883.
52. Izuka, A.; Winter, H. H.; Hashimoto, T. Macromolecules 1992, 25, 2422.
53. Pryde, C. A. J Polym Sci A Polym Chem 1993, 31, 1045.
54. Siani, A. K.; Carlin, C. M.; Patterson, H. H. J Polym Sci A, Polym Chem 1993, 31, 2751.
55. Aoki, Y.; Li, L.; Uchido, H.; Kakiuchi, M.; Watanabe, H. Macromolecules 1998, 31, 7472.
56. Muthukumar, M. Macromolecules 1989, 27, 17.
57. Duran, D.; Delsanti, M.; Adam, M.; Luck, J. M. Europhys Lett 1987, 3, 97.